JOURNAL OF MATERIALS SCIENCE **38** (2003) 1535– 1542

Improvement of creep-fatigue life by the modification of carbide characteristics through grain boundary serration in an AISI 304 stainless steel

HYUN UK HONG, SOO WOO NAM*
Department of Materials Science and Engineering, Korea Advanced Institute of Science and Technology, 373-1 Kusong-dong, Yusong-gu, Taejon 305-701, South Korea
E-mail: namsw@cais.kaist.ac.kr

The modification of carbide characteristics through grain boundary serration and its subsequent effect on the creep-fatigue property at 873 K have been investigated, using an AISI 304 stainless steel. It was found that the grain boundaries are considerably serrated when a specimen is furnace-cooled. The grain boundary serration leads to a change in the carbide characteristics as well as grain boundary configuration, i.e., morphology of carbide from an acute triangular to a planar form and a lowered density. Additionally, an array of carbide particles is changed from a consistent to zigzag pattern, in terms of their preference to one grain to share the coherency. Planar carbides on serrated grain boundaries have a lower interfacial energy than that of triangular carbides on straight grain boundaries. It is suggested that the modification of carbide characteristics through the grain boundary serration has a remarkable influence on the improvement of creep-fatigue resistance.

1. Introduction

Austenitic stainless steels are of interest as structural materials for elevated temperature applications in power generation and chemical industries. For these applications, components of a structure are subjected to complex stress-loading cycles at high temperature. Thus, understanding of the damaging process of high temperature creep-fatigue failure is of great importance to the optimum design of the components for improvement of reliability.

It has been well established that grain boundary cavitation is the most serious damage mechanism of austenitic stainless steels under creep-fatigue interaction conditions [1–6]. The carbides at the grain boundaries provide preferential sites for cavity nucleation owing to stress concentration during the fatigue cycle [2–6]. Hence, these carbide characteristics, such as distribution, density and morphology, etc., should be considered as important factors to determine creep-fatigue property. Yoon and Nam [4, 5] confirmed that a higher density of carbide is more likely to lead to shorter creep-fatigue life and a higher cavity nucleation factor, P'. Careful observations also inform that different carbide shapes and distribution between 304 and 316 stainless steels resulted in different types of fractured surfaces as a result of different cavitation behaviors [7, 8].

Recently, the present authors [9] found that grain boundary serration in 316 stainless steel occurs in an early stage of the aging treatment prior to the $M_{23}C_6$ carbides precipitation. Moreover, they emphasized that the grain boundary serration strongly affects the density of carbide and its morphology. It was suggested that modified grain boundary carbides may be favorable for the cavity resistance of austenitic stainless steels during creep-fatigue conditions. An explanation on the mechanism for the occurrence of grain boundary serration in the view of thermodynamics has been proposed by the authors [10]. The occurrence of grain boundary serration originates from the minimization of total free energy of a material at a given temperature, and the serrated grain boundaries can be considered as the stable configuration formed at a lower temperature while the straight grain boundaries are that at a higher temperature.

This proposed mechanism for the grain boundary serration is fundamentally different from ones in the Ni-base superalloys [11, 12] in the viewpoint that the serration occurs spontaneously without the presence of precipitates. However, further investigation should be made to identify the grain boundary microchemistry after serration [12] so that the more systematic and reliable mechanism for the

*Jointly appointed at the Center for the Advanced Aerospace Materials, Pohang University of Science and Technology, San 31 Hyoja-dong Nam-gu, Pohang, 790-784, South Korea.

0022–2461

grain boundary serration of 316 stainless steel can be proposed.

It has been reported that no grain boundary serration occurs in 304 stainless steel so that acute triangular carbides formed on the straight grain boundaries are predominant [13]. In this study, a modified heat treatment for an AISI 304 stainless steel to obtain serrated grain boundaries is proposed and applied. The dependency of carbide characteristics on grain boundary serration is discussed. Furthermore, the effect of the modification of carbide characteristics through the grain boundary serration has been investigated in terms of the improvement of creep-fatigue resistance.

Early studies simply concentrated on the correlation of grain boundary configuration with the creep or fatigue property, without considering the characteristics of precipitates on grain boundaries [14–16]. They stated that the improvement of creep or fatigue strength was directly related with the retardation of grain boundary sliding in terms of the serrated grain boundaries. However, it is shown in this investigation that there is little indication that grain boundary sliding is prevailing.

2. Experimental procedure

2.1. Heat treatment design for the grain boundary serration

The chemical composition of the investigated AISI 304 stainless steel is given in Table I. The steel shows triangular carbides on the straight grain boundaries as long as it is conventionally heat-treated (304-T), as shown in Fig. 1a. In order to have the occurrence of grain boundary serration, several required conditions can be proposed on the basis of previous results [9, 10]: Grain boundary carbide precipitation should be retarded as much as possible, since carbide particles may inhibit the boundary movement as pinning points (note that the grain boundary serration occurs prior to carbide precipitation); Sufficient temperature and time should be provided for the grain boundaries to move easily; A thermal equilibrium state should be continuously maintained during cooling from a higher solution to a lower aging treatment temperature, since grain boundary serration is known to occur spontaneously [10, 17, 18].

The above conditions can be simultaneously satisfied by cooling the specimen as slowly as possible during the heat treatment. Thus, a modified heat treatment was designed to have the occurrence of grain boundary serration, as shown in Table II. The modified heat-treated steel has planar carbides on the serrated grain boundaries (304-P), as shown in Fig. 1b. This finding indicates that the grain boundaries are considerably serrated when a specimen is furnace-cooled. Fig. 2 shows the sequential development of grain boundary serration and subsequent carbide precipitation.

TABLE I The chemical composition of the investigated AISI 304 stainless steel

C	Si	Mn	P	S	Cr	Ni	Mo
0.077	0.5	1.5	0.02	0.016	18.2	8.3	0.2

All in wt%.

TABLE II Heat treatment of steel

Specimens	Heat treatment[a]
304-T (conventional)	1323 K/1 h/WQ + 1033 K/50 hr/WQ
304-P (modified)	1323 K/1 h → FC → 1033 K/50 h/WQ

Both the steels have a same grain size of about 50 μm after the heat treatment.
[a]WQ: water-quenched (~360 K/sec), FC: furnace-cooled (~4 K/min).

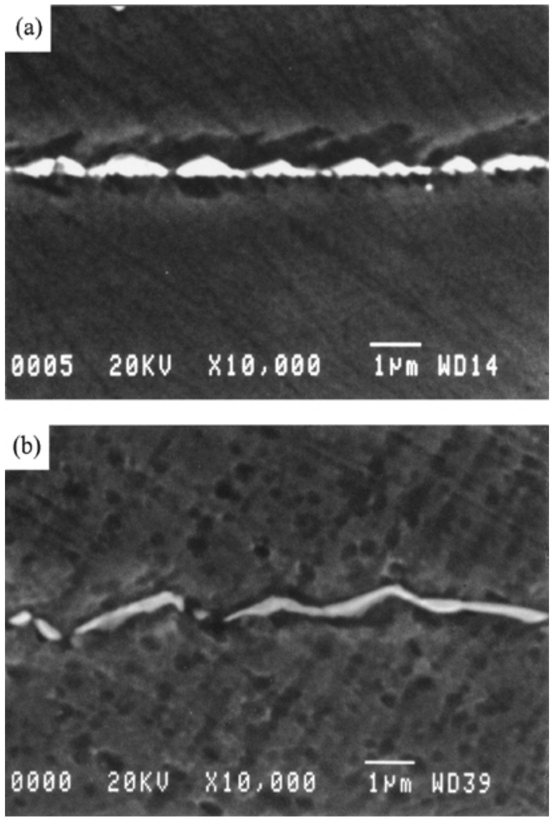

Figure 1 SEM micrographs showing the grain boundary carbides: (a) triangular carbides on the straight grain boundary (304-T) and (b) planar carbides on the serrated grain boundary (304-P).

2.2. Microstructures characterization

The characterization of grain boundary misorientation and the orientation relationship between a carbide and two neighboring grains were carried out in a scanning electron microscope (SEM) Philips XL30 field emission gun (FEG) utilizing electron backscattered diffraction (EBSD) technique. A transmission electron microscope (TEM) was used to obtain crystallographic features (Jeol JEM-3010 operating at 300 kV). TEM foils were prepared by the twin-jet method using 5 vol% perchloric acid + 95 vol% acetic acid at 288 K, 30 V.

2.3. Low cycle fatigue testing

Round specimens with a diameter of 7 mm and a gauge length of 8 mm were used to conduct total strain-controlled creep-fatigue tests, with a strain rate of 4×10^{-3}/s in air atmosphere at 873 K. The hold time at the tensile peak strain was 10 min. All the data including the hysteresis loop energy were recorded using a computer data acquisition system.

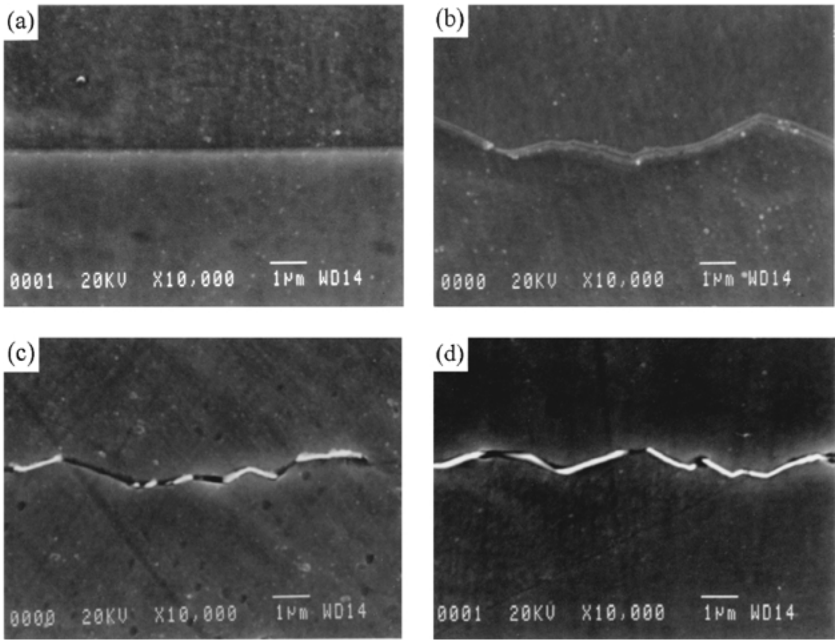

Figure 2 The sequential development of grain boundary serration and subsequent carbide precipitation: (a) after solution-treated (1323 K/1 h/WQ), (b) after furnace-cooled to 1033 K and aged for 5 min, (c) after furnace-cooled to 1033 K and aged for 15 min, and (d) after furnace-cooled to 1033 K and aged for 3 hr.

3. Results and discussion

3.1. Comparison of carbide characteristics (the dependency of carbide characteristics on the grain boundary serration)

As shown in Fig. 1, it is observed that the carbide morphologies are triangular in 304-T and planar in 304-P. The linear densities of the carbides, which were measured by an image analyzer with SEM micrographs, are 2.6×10^3/cm in 304-T and 0.7×10^3/cm in 304-P, respectively. These different carbide characteristics between the two steels are attributed to the grain boundary serration. Thus, it can be said that the grain boundary serration leads to a change in the carbide characteristics as well as grain boundary configuration, i.e., morphology from an acute triangular to a planar form and a lowered density of carbides.

Trace analysis was used to identify the interfaces of the carbides in the two steels. The result is shown in Fig. 3. A coherent carbide interface was revealed to be $(11\bar{1})$ in both steels, while the incoherent interfaces were different, i.e. (200) and $(02\bar{2})$ in the case of 304-T and $(11\bar{1})$ in 304-P. It is noteworthy that the incoherent interface of planar carbide in 304-P is observed to be exactly parallel to the coherent interface, i.e. $(11\bar{1})$. It is expected that the planar carbides of 304-P possess a lower interfacial energy than that of the triangular carbides of 304-T, since they have a lower indices of interfaces, associated with the closely packed plane [13, 19]. Therefore, planar carbides may be favorable for cavitation resistance.

EBSD technique was used to investigate the orientation relationship between a carbide particle and two neighboring grains. Comparison of the array of carbide particles between the two steels was made in terms of their preference to one grain in order to share the coherency. Fig. 4a shows representative triangular carbides at the straight grain boundary. It can be seen that all the carbides are in parallel orientation to grain 1. From all the Kikuchi patterns obtained from the individual carbide particles (identified by ‘1’), it is clearly identical to that of grain 1. On the other hand, in the case of planar carbides formed at the serrated grain boundary, as shown in Fig. 4b, some carbides are in

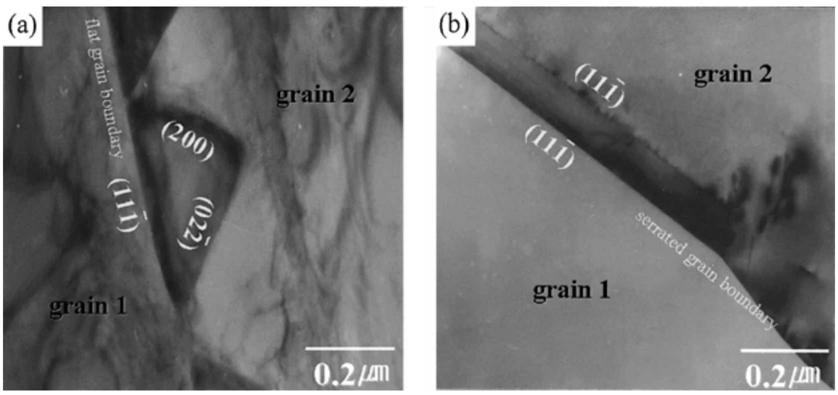

Figure 3 TEM micrographs showing the interfacial planes of the grain boundary carbide: (a) 304-T and (b) 304-P.

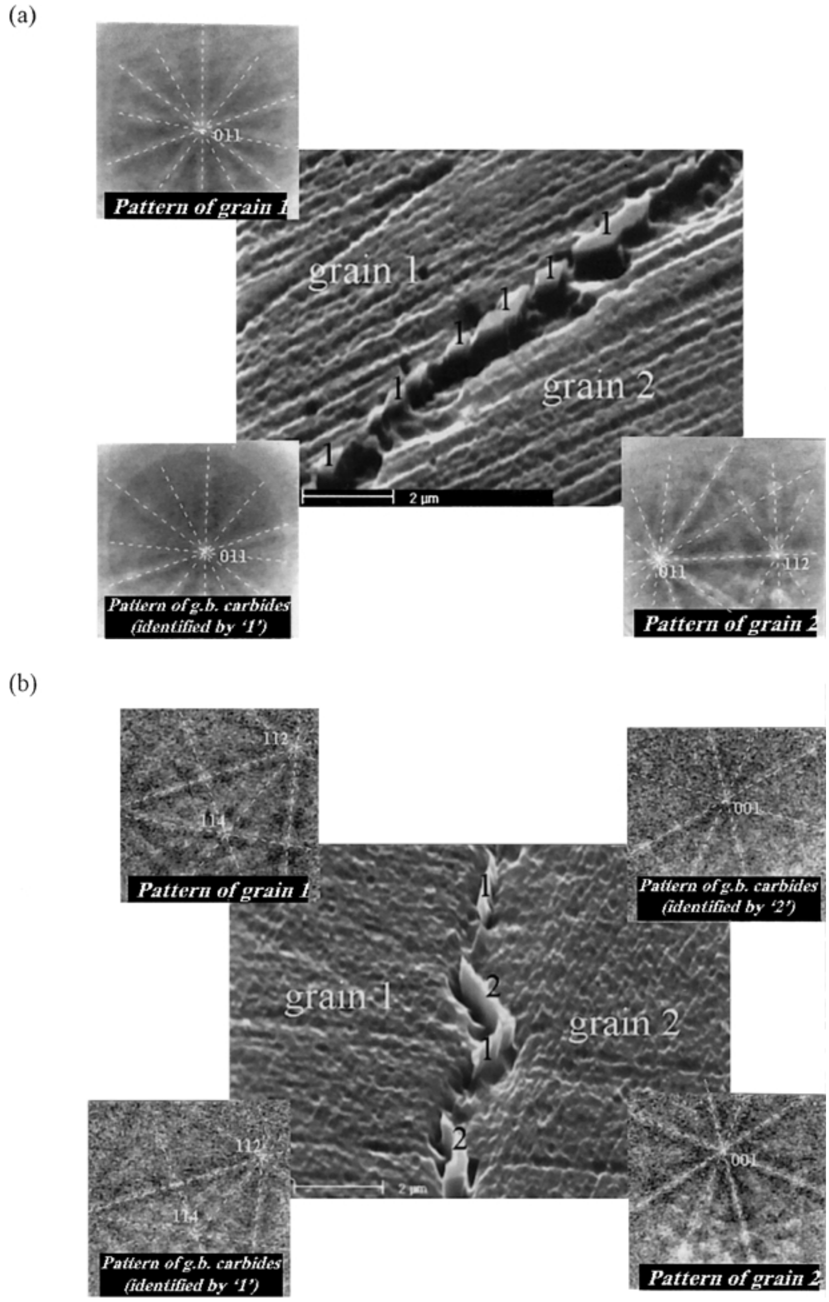

Figure 4 Comparison of the array of carbide particles in terms of their preference to one grain in order to share the coherency: (a) 304-T and (b) 304-P. Note the Kikuchi patterns illustrating each carbide oriented parallel to grain 1 or grain 2.

parallel orientation with grain 1 and some with grain 2 even though they precipitate at the same grain boundary. From these results, it can be confirmed that grain boundary serration leads to the development of an array of carbide particles from a consistent to zigzag pattern, as well as influencing carbide density and morphology. Additionally, it can be known that grain boundary carbides of 304 SS can be modified to be similar with those of 316 SS [9] by the introduction of serration.

3.2. Comparison of tensile properties

Table III shows the results of tensile tests at 873 K for the two steels. Both steels have almost similar tensile properties. This implies that carbide modification through the grain boundary serration has little influence on the fundamental mechanical properties.

3.3. Comparison of creep-fatigue resistances

Fig. 5 shows a comparison of low cycle fatigue resistances of both steels at 873 K. Under continuous fatigue tests, the two steels show similar fatigue resistance. This result is understood to be because of the fact that the major fatigue damage under this condition is surface crack formation and its transgranular propagation. However, under creep-fatigue conditions, where the main damage is known to be grain boundary cavitation, the life of 304-P is almost twice as long

TABLE III Summary of tensile properties of the two steels at 873 K

Specimens	YS (MPa)	UTS (MPa)	Elongation (%)
304-T	149	379	40.0
304-P	153	383	39.6

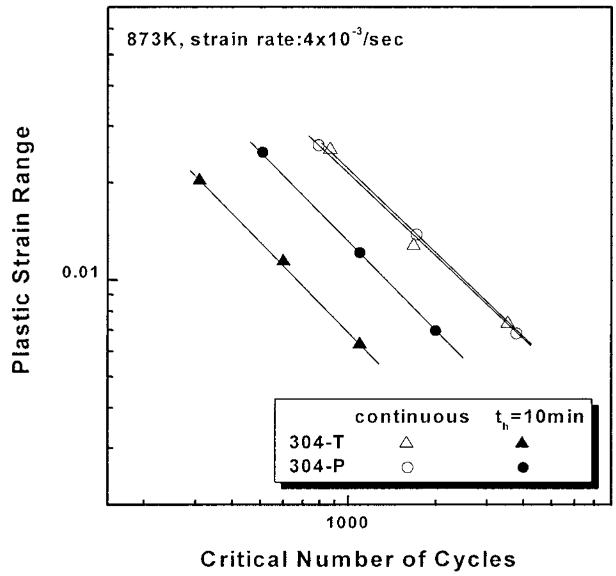

Figure 5 Comparison of low cycle fatigue resistances of the two steels at 873 K.

as that of 304-T. This indicates that the creep-fatigue resistance of 304 stainless steel can be remarkably improved by the introduction of grain boundary serration and the subsequent modification of carbide characteristics. This result is also consistent with earlier studies finding that grain boundary cavitation is the main damage process in austenitic stainless steels under tensile hold creep-fatigue interaction conditions, and this cavitation behavior (or creep-fatigue property of a given material) is closely related with the characteristics of grain boundary carbides.

After the creep-fatigue tests, the specimen gauge was sectioned in a longitudinal direction parallel with the stress axis. Fig. 6 shows the microstructures of the two

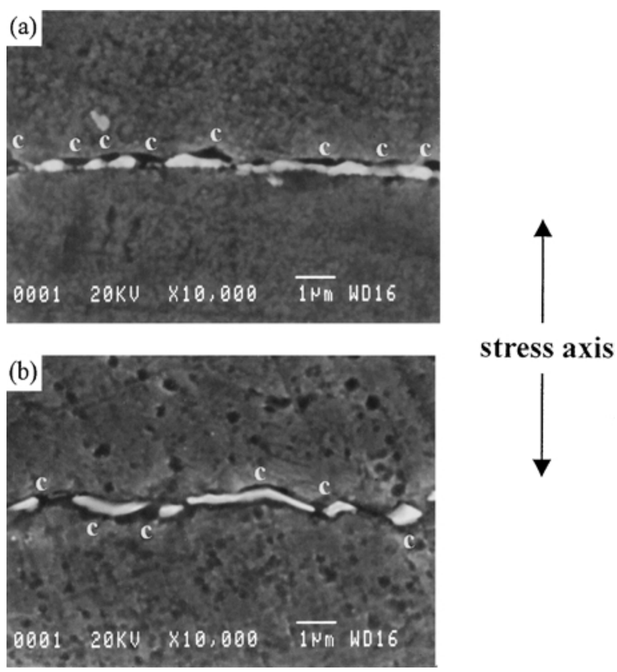

Figure 6 Longitudinal sections showing the grain boundary carbides and cavities after the creep-fatigue test: (a) 304-T and (b) 304-P. Cavities are indicated by 'c'.

steels. It is seen that the array of cavities formed on the interfaces of carbide particles is consistent to one side in 304-T while it forms on either side in 304-P. This result can be explained by the fact that the two steels have different arrays of coherent interfaces of carbides, as stated earlier.

Figs 7 and 8 show the fractured surfaces of 304-T and 304-P, respectively. The pair of grain boundary facets matches together. In the case of 304-T, it is clear that only cavities are observed on one side of the grain boundary facet (Fig. 7b), and only carbides on the opposite side of the grain boundary facet (Fig. 7d). Each cavity corresponds with each carbide in a one to one manner. On the other hand, in the case of 304-P, the grain boundaries consist of facets containing steps, as clearly shown in Fig. 8. It is observed that carbides and cavities coexist on one side of the grain boundary facet (Fig. 8b or d).

3.4. Comparison of cavity nucleation factor, P′

Recently, Nam *et al.* [4, 5] proposed a life prediction model, which can predict the accurate fatigue life under creep-fatigue condition in materials whose failure is controlled by grain boundary cavitational damage. It is also observed that the prediction model is applicable to this present work because of the good agreement between experimental and predicted lives. This model rationalizes that vacancies are formed athermally by plastic deformation during fatigue cycle and cluster to form cavities at the grain boundaries. Also, it is assumed that the number of cavities in a cycle is proportional to the plastic strain range. Therefore, the number of nucleated cavities during cyclic loading per unit area of grain boundary, n, is formulated to be

$$n = P'\Delta\varepsilon_p N \qquad (1)$$

where P', $\Delta\varepsilon_p$ and N are the linear constant for cavity nucleation, the plastic strain range, and the number of cycles, respectively. They suggested that P', the cavity nucleation factor, is regarded as the ease of cavity nucleation and verified that smaller P' value results in more retardation of cavitation to increase creep-fatigue resistance. Moreover, the P' value of each steel is associated with the characteristics of grain boundary precipitates (density and morphology) acting as cavity nucleation sites.

Using this concept, comparison of the cavity nucleation factor, P', for this investigation is made for the two steels. The values of P' are evaluated to be 4.7×10^{12} m^{-2} in 304-T and 2.9×10^{12} m^{-2} in 304-P. It is found that 304-P has a lower P' value than that of 304-T. This result is closely related with the difference in creep-fatigue lives, i.e., 304-P shows almost twice-longer life than that of 304-T. This implies that the carbide modification through the grain boundary serration, which can be quantified as P' value, leads to improvement of cavitation resistance for the enhancement of creep-fatigue property.

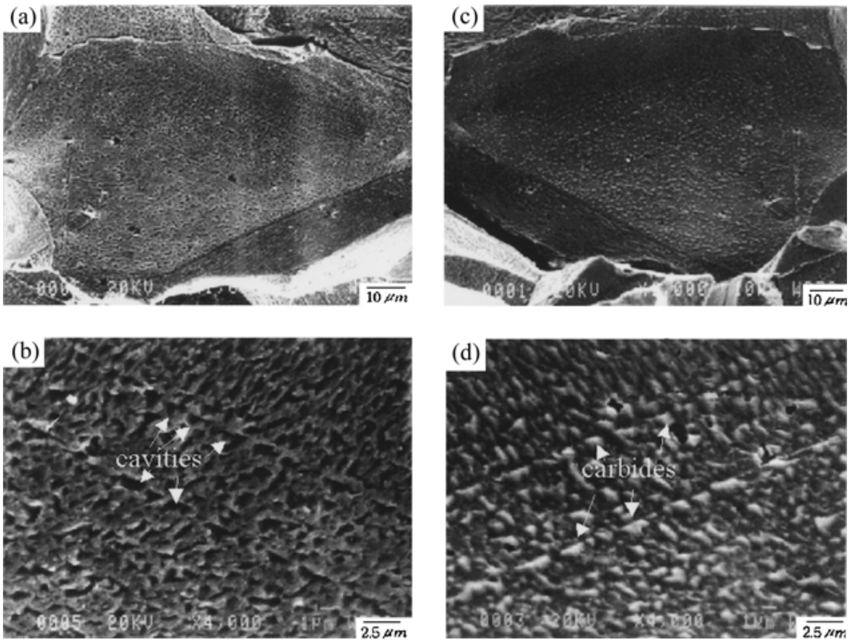

Figure 7 SEM micrographs showing a pair of fractured surfaces of 304-T after the creep-fatigue test ($T = 873$ K, $\Delta\varepsilon_t = \pm 2.0\%$, $t_h = 10$ min): (a) cavities on one side of the grain boundary facet, (b) highly magnified observation of (a), (c) carbides on the other side of the grain boundary facet, and (d) highly magnified observation of (c).

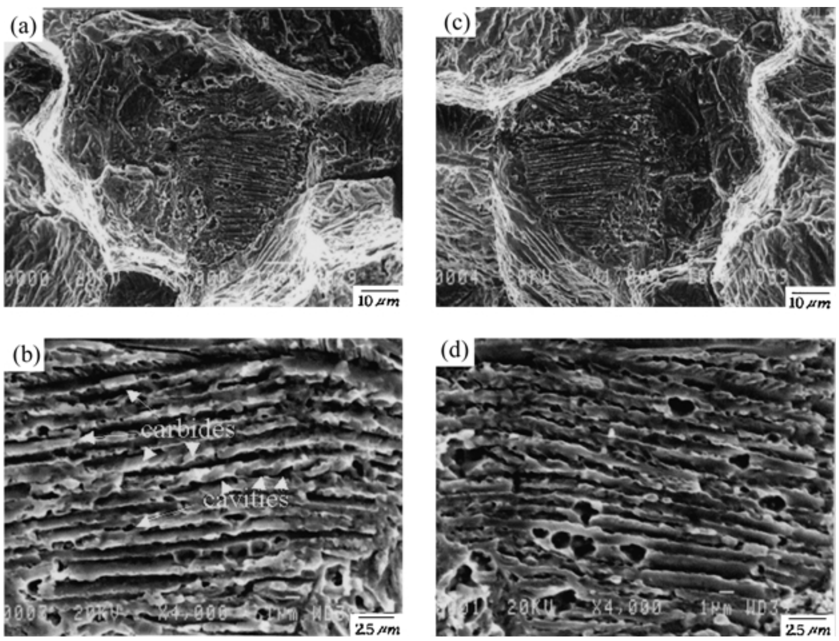

Figure 8 SEM micrographs showing a pair of fractured surfaces of 304-P after the creep-fatigue test ($T = 873$ K, $\Delta\varepsilon_t = \pm 2.0\%$, $t_h = 10$ min): (a) low magnification of one side of the grain boundary facet, (b) highly magnified observation of (a), (c) low magnification of the other side of the grain boundary facet, and (d) highly magnified observation of (c). Note that carbides and cavities coexist on the same grain boundary facet. The grain boundaries consist of facets containing steps.

4. Discussion

The creep-fatigue life of 304 stainless steel at 873 K is remarkably improved by the introduction of the modified heat treatment for the grain boundary serration. The grain boundary serration involves a change of carbide characteristics as well as boundary morphology. Thus, we need to make it clear which one is the main contribution to the improvement of creep-fatigue resistance, i.e., the modification of grain boundary carbides or the serrated grain boundary itself.

Many researchers [14–16] demonstrated that the improvement of creep or fatigue strength resulted from the retardation of grain boundary sliding in terms of the serrated grain boundaries. Consequently, they simply concentrated on the correlation of grain boundary configuration with the creep or fatigue property. In this study, the presence of damage from grain boundary sliding is considered first.

It has been well known that stress concentrations can be produced at the particle/matrix interface when sliding occurs in a boundary containing second phase particles [20]. Under this situation, in which grain boundary sliding is the main damage process for grain boundary cavitation, maximum cavitation will occur on those grain boundaries oriented so as to experience the greatest shear stress, i.e., boundaries at angles of approximately 45° with respect to the stress axis.

However, in this investigation it is observed that the boundaries, which are perpendicular to the stress axis, are more susceptible to cavitational damage than the ones inclined to the stress axis in both steels subjected to a creep-fatigue test ($T = 873$ K, $\Delta\varepsilon_t = \pm 2.0\%$, hold time at the tensile peak strain = 10 min), as shown in Fig. 9. Fig. 10 shows the angular distribution of the cavitated grain boundaries with respect to the stress axis. The examined area was a gauge section of a specimen and the count criterion was that the cavitated length of a grain boundary should be more than 10 μm. From Fig. 10 it can be seen that the level of cavitation is definitely highest on boundaries making an angle of around 90° with respect to the stress axis. This seems to be different with previous investigations reporting that grain boundary sliding is important in the cavitation process. Furthermore, wedge cracks and elongated cavities, which are frequently observed at the grain boundaries or triple junctions when grain boundary sliding actively occurs, were rarely observed in this investigation (see Fig. 6). Several researchers [21, 22], as well as the present authors, have shown that under compressive hold creep-fatigue interaction conditions, no cavitational damage can be found on grain boundaries, resulting in almost no reduction of life when comparing continuous fatigue life. Nam *et al.* [6] found no sign of grain boundary sliding from the result that there was no shift of straight lines across the grain boundary. Therefore, from these series of results, it can be confirmed that there is little indication that cavity formation is mainly due to the grain boundary sliding. From this finding, it is to be expected that the improvement of creep-fatigue resistance by serration would largely result from the modification of grain boundary carbides rather than grain boundary configuration.

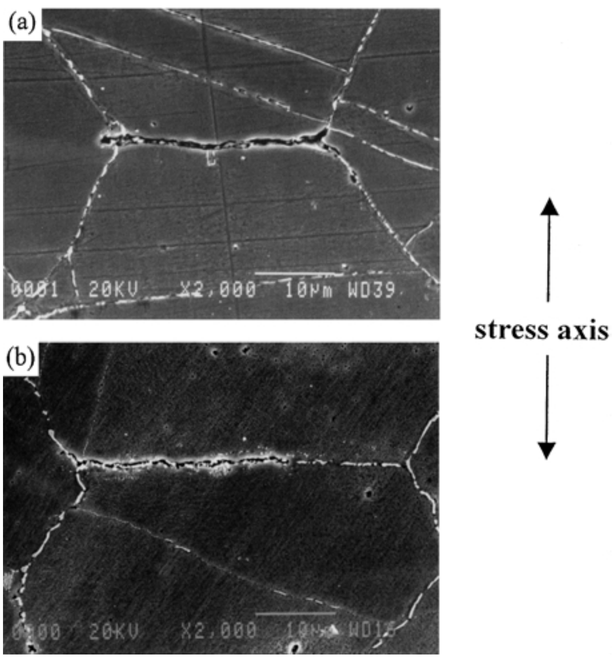

Figure 9 Longitudinal sections showing the grain boundaries of (a) 304-T and (b) 304-P after the creep-fatigue test. Cavitational damage is much more pronounced on the perpendicular grain boundary than the inclined ones in both steels.

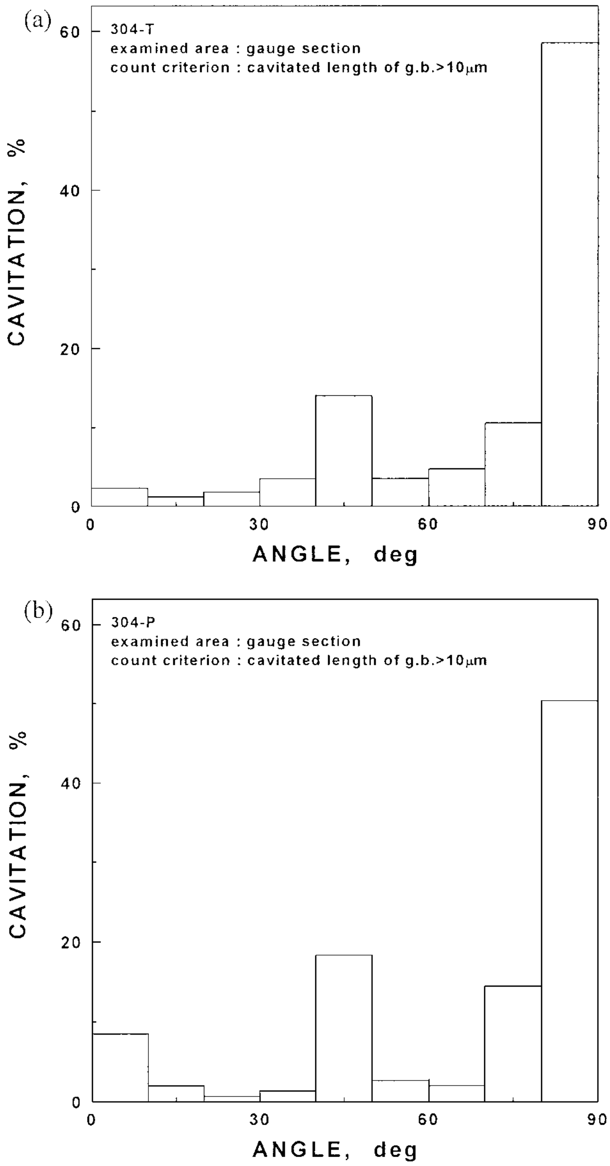

Figure 10 Angular distribution of cavitated grain boundaries with respect to the stress axis: (a) 304-T and (b) 304-P.

Further evidence to support the above mentioned argument is presented by conducting a special experiment. One specimen having straight grain boundaries without carbides (see Fig. 2a) and another having serrated grain boundaries without carbides (see Fig. 2b) were prepared. Creep-fatigue tests were then conducted at 873 K, using these two kinds of steels. The results are summarized in Table IV. Both steels show almost similar creep-fatigue properties except that the specimen

TABLE IV Summary of creep-fatigue properties of the two steels, which contain no carbides before the test. The values (except the life) were taken at the half cycles of failure

Specimens	$\Delta\sigma_{max}$ (MPa)	$\Delta\sigma_{min}$ (MPa)	$\Delta\varepsilon_p$	$\int \sigma dt$ (MPa · sec)	Hysteresis loop area (MJ/m^3)	Cycles to failure
Straight GBs	331	−351	0.0217	125431	13.1	201
Serrated GBs	329	−347	0.0226	124710	12.8	253

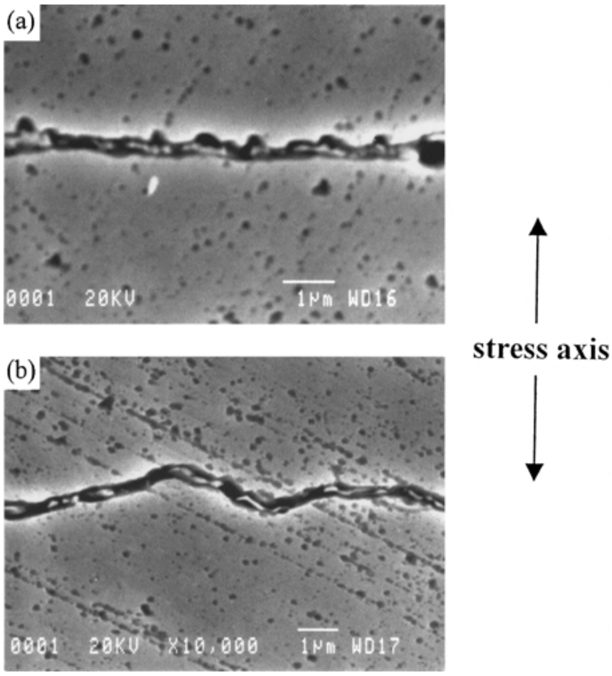

Figure 11 Longitudinal sections showing the grain boundary carbides and cavities after the creep-fatigue test: (a) specimen having straight grain boundaries and (b) specimen having serrated grain boundaries. Note that the carbide size and morphology are observed to be similar in both the steels.

having serrated grain boundaries has somewhat longer life than the one having straight grain boundaries. However, the difference in life between the two steels appears to be not so significant when comparing the extent of improved life obtained from 304-T and 304-P (304-P has 2 times longer life than that of 304-T). During the creep-fatigue test, the carbides precipitate dynamically on the grain boundaries in both steels. It is generally accepted that these carbides formed dynamically at the early stage of cycles provide the preferential site for cavity nucleation [6]. Fig. 11 shows the longitudinal sections of the two steels after the test. The dynamically formed carbides of both steels are seen to be the same in terms of distribution and morphology, regardless of grain boundary shape. Thus, it is concluded that the improvement of creep-fatigue resistance cannot be remarkably attained only by the grain boundary shape effect without considering the modification of carbide characteristics.

5. Conclusion

1. The modification of carbide characteristics (density, morphology and array) through grain boundary serration can be obtained by furnace-cooling heat treatment.

2. Grain boundary serration leads to a change in the carbide characteristics, i.e., morphology from an acute triangular to a planar form, lowered density and an array of carbide particles from consistent to zigzag pattern when carbides prefer to one grain in order to share coherency. Planar carbides on serrated grain boundaries have a lower interfacial energy than that of triangular carbides on straight grain boundaries.

3. The creep-fatigue resistance can be remarkably improved by the modification of carbides through grain boundary serration. This result is understood in light of that the modified carbides, whose interface energy is lower, have higher cavitation resistance, resulting in the retardation of cavity nucleation and growth to increase creep-fatigue life.

4. It is confirmed that the cavity nucleation factor, P′ value, is closely associated with the characteristics of grain boundary carbides (density, morphology and array) acting as cavity nucleation sites.

5. This modified heat treatment procedures proposed in this investigation can be directly applied to the practical industrial use.

References

1. P. S. MAIYA, *Mater. Sci. Eng.* **47** (1981) 13.
2. J. W. HONG, S. W. NAM and K.-T. RIE, *J. Mater. Sci.* **20** (1985) 3763.
3. S. W. NAM, J. W. HONG and K.-T. RIE, *Metall. Trans.* A **19A** (1988) 121.
4. B. G. CHOI, S. W. NAM, Y. C. YOON and J. J. KIM, *J. Mater. Sci.* **31** (1996) 4957.
5. S. W. NAM, Y. C. YOON, B. G. CHOI, J. M. LEE and J. W. HONG, *Metall. Mater. Trans.* A **27A** (1996) 1273.
6. J. M. LEE and S. W. NAM, *Int. J. Damage. Mech.* **2** (1993) 4.
7. S. W. NAM, S. C. LEE and J. M. LEE, *Nucl. Eng. Design* **153** (1995) 213.
8. B. G. CHOI, S. W. NAM and J. GINSZTLER, *J. Mater. Sci.* **35** (2000) 1699.
9. H. U. HONG and S. W. NAM, *Mater. Sci. Eng.* A **332** (2002) 255.
10. *Idem., Z. Metallkd.* **92** (2001) 12.
11. J. M. LARSON and S. F. FLOREEN, *Metall. Trans.* A **8** (1977) 51.
12. L. LETELLIER, M. GUTTMANN and D. BLAVETTE, *Phil. Mag. Letters* **70** (1994) 189.
13. H. U. HONG, B. S. RHO and S. W. NAM, *Mater. Sci. Eng.* A **318** (2001) 285.
14. T. SAEGUSA and J. R. WEERTMAN, *Scripta Metall.* **12** (1978) 187.
15. H. IIZUKA, M. TANAKA, O. MIYAGAWA and D. FUJISHIRO, in Proceedings of 4th JIM International Symposium on Grain Boundary Structure and Related Phenomena, Minakami, Japan, November 1985, edited by Seiichi Karashima (The Japan Institute of Metals, 1985) p. 851.
16. M. TANAKA, H. IIZUKA and F. ASHIHARA, *Trans. ISIJ* **28** (1988) 129.
17. J. W. CAHN, *J. Physique* **43** (1982) 199.
18. T. E. HSIEH and R. W. BALLUFFI, *Acta Metall.* **37** (1989) 2133.
19. S. HIRTH and G. GOTTSTEIN, *Acta Mater.* **46** (1998) 3975.
20. J. WEERTMAN, *Metall. Trans.* **5** (1974) 1743.
21. C. Y. CHENG and D. R. DIERKS, *ibid.* A **4A** (1973) 615.
22. S. MAJUMDAR and P. S. MAIYA, *J. Eng. Mater. Tech.* **102** (1980) 159.

Received 5 December 2001
and accepted 24 December 2002